

Redox Non-innocent Ligand Controls Water Oxidation Overpotential in a New Family of Mononuclear Cu-Based Efficient Catalysts

Pablo Garrido-Barros,[†] Ignacio Funes-Ardoiz,[†] Samuel Drouet,[†] Jordi Benet-Buchholz,[†] Feliu Maseras,^{*,†,‡} and Antoni Llobet^{*,†,‡}

[†]Institute of Chemical Research of Catalonia (ICIQ), Avda. Països Catalans, 16, 43007 Tarragona, Spain

[‡]Departament de Química, Universitat Autònoma de Barcelona, 08193 Bellaterra, Spain

Supporting Information

ABSTRACT: A new family of tetra-anionic tetradentate amidate ligands, N_1, N_1' -(1,2-phenylene)bis(N_2 -methyl-oxalamide) (H_4L1), and its derivatives containing electron-donating groups at the aromatic ring have been prepared and characterized, together with their corresponding anionic Cu(II) complexes, $[(LY)Cu]^{2-}$. At pH 11.5, the latter undergoes a reversible metal-based III/II oxidation process at 0.56 V and a ligand-based pH-dependent electron-transfer process at 1.25 V, associated with a large electrocatalytic water oxidation wave (overpotential of 700 mV). Foot-of-the-wave analysis gives a catalytic rate constant of 3.6 s^{-1} at pH 11.5 and 12 s^{-1} at pH 12.5. As the electron-donating capacity at the aromatic ring increases, the overpotential is drastically reduced down to a record low of 170 mV. In addition, DFT calculations allow us to propose a complete catalytic cycle that uncovers an unprecedented pathway in which crucial O–O bond formation occurs in a two-step, one-electron process where the peroxo intermediate generated has no formal M–O bond but is strongly hydrogen bonded to the auxiliary ligand.

Molecular water oxidation catalysis by transition metal complexes¹ is a highly active field of research at present due to its implications in new energy conversion schemes based on splitting water with sunlight.² In addition, water oxidation is also of interest in biology because it is the reaction that takes place at the oxygen-evolving complex of photosystem II in green plants and algae.³ The very high thermodynamic potential needed for water oxidation (1.23 V vs NHE at pH 0.0) implies necessarily the use of transition metal complexes containing oxidatively rugged ligands, in order to come up with long-lasting systems that can have potential commercial applications.^{2c,4} In addition, these complexes need to work in water as a solvent, imposing an additional requirement for the auxiliary ligands to be substitutionally inert at the pH of action; otherwise, they end up generating the corresponding aqua/hydroxo complexes and the free ligand. This is especially critical for first-row transition metal complexes, as has been previously shown in the literature,⁵ because there will only be a limited pH range where the integrity of the complex is maintained. Furthermore, ligand liberation from the metal complex is an additional driving force toward the formation of metal oxides and/or mixed oxo-hydroxides that will be highly dependent on

working pH. On the other hand, an interesting feature of water oxidation catalyst (WOC) design is the use of redox non-innocent ligands that can help with the difficult task of managing the multiple protons and multiple electrons transfers needed to carry out the water oxidation reaction.⁶ This feature would be particularly useful if the ligand-based redox processes are tied to the rate-determining step (rds) of the catalytic process and not linked to unwanted radical-based reactions leading to fast decomposition.⁷

In order to explore the options for water oxidation catalysis based on oxidatively rugged but redox-active ligands, we have prepared a family of four Cu(II) complexes containing the tetradentate amidate acyclic ligands H_4LY ($Y = 1-4$) with different substituent groups at the aromatic ring (see Figure 1). The H_4LY ($Y = 2-4$) ligands are new compounds that have been prepared following related procedures already described for the unsubstituted ligand H_4L1 .⁸

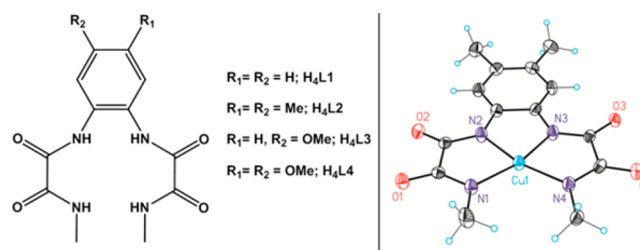


Figure 1. (Left) Ligand structures and (right) ORTEP figure of complex $[(L2)Cu]^{2-}$.

The new copper complexes reported here, $[(LY)Cu](NMe_4)_2$ ($Y = 2-4$), have been characterized by the usual spectroscopic techniques and by monocrystal X-ray diffraction analysis. An ORTEP view of the cationic part of complex $[(L2)Cu](NMe_4)_2$ is depicted in Figure 1, while those for the other methoxy derivatives are presented in the Supporting Information (SI). It is interesting to observe here that the d^9 Cu(II) ion is four-coordinate with a basically square planar geometry, manifesting the existence of π -delocalization over the phenyl and amidate moieties of the ligand and ensuring strong ligand bonding to the metal center.

Received: April 17, 2015

Published: May 18, 2015

The redox properties of the anionic complexes $[(LY)Cu]^{2-}$ ($Y = 1-4$) were investigated by cyclic voltammetry (CV) and amperometric techniques using a mercury sulfate reference electrode saturated with K_2SO_4 (MSE) unless explicitly indicated. All redox potentials in the present work are reported versus NHE by adding 0.65 V to the measured potential. Figure 2 shows the CV experiments carried out for $[(L1)Cu]^{2-}$ in the pH range 11.5–12.5.

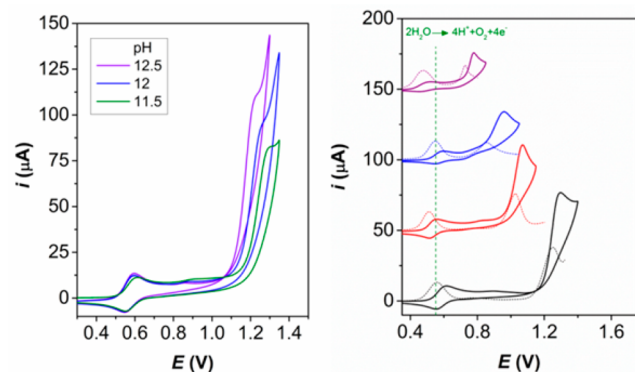
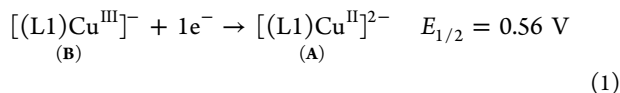


Figure 2. (Left) CV experiments with 1 mM $[(L1)Cu]^{2-}$ in phosphate buffer (0.1 M of ionic strength) at different pH values. (Right) CV and DPV for complexes $[(LY)Cu]^{2-}$ ($Y = 1-4$). The green vertical dashed line indicates the thermodynamic E° for the $4e^-$ oxidation of water to dioxygen at pH 11.5. CVs are run at a scan rate of 100 mV/s.

A first pH-independent, chemically reversible, and electrochemically quasi-reversible wave at $E_{1/2} = 0.56$ V vs NHE ($\Delta E = 71$ mV), eq 1, is associated with the formation of a d^8 Cu(III)



square planar ion with very low reorganizational energy, as inferred from the very small differences in their respective geometries, and with a relatively low potential due to the tetra-anionic nature of the L1 ligand (the A and B labels indicated here are also used in Figure 3). A second pH-dependent wave (approximately 59 mV/pH unit) observed at more anodic potentials, eq 2, is associated with a ligand-based aryl oxidation,

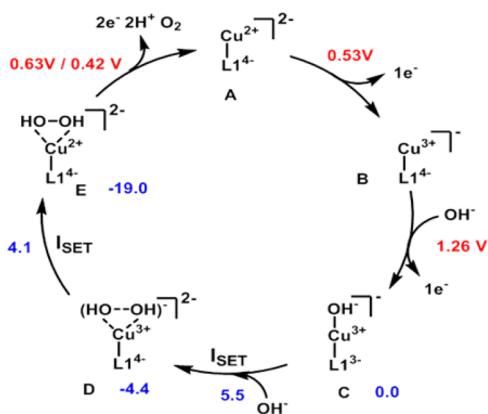
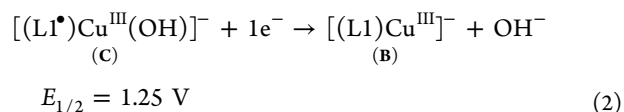


Figure 3. Calculated catalytic cycle. Free energy changes for steps at the electrode are indicated explicitly in volts (red) and for steps in solution are indicated in kcal/mol (blue).



forming formally a phenyl radical cation, together with the coordination of a hydroxido ligand. This ligand-based oxidation had been previously proposed on electrochemical grounds for related complexes⁹ and is further supported by the strong inductive effects exerted by the phenyl substituents, as will be shown further below and also supported by DFT calculations (*vide infra*). In the presence of water, this wave is associated with a large electrocatalytic anodic current due to the catalytic oxidation of water to dioxygen.

In order to obtain kinetic information about the catalytic process, a foot-of-the-wave analysis (FOWA) was carried out to calculate the apparent rate constant, k_{obs} . We followed the methodology described in the literature,¹⁰ assuming that the rds is the last electron-transfer step coupled to a chemical reaction. The largest slope at the very beginning of the catalytic process gives an impressive value of $k_{obs} = 3.56 \text{ s}^{-1}$ that is basically independent of the scan rate and thus in agreement with the model proposed. These kinetic values compare well with the ones reported in the literature for related complexes (see Table 1, below). However, since different methods are used for this type of calculation, the comparisons should be done with caution.

To confirm the stability of the WOCs, spectroelectrochemical experiments were performed using an OTTLE cell, scanning from 0.4 to 1.25 V and back to the original 0.4 V at a very low scan rate of 2 mV/s that allows for complete transformations during the redox events. Under these conditions, the initial complex is fully recovered, as ascertained by both UV–vis spectroscopy and charge integration under the III/II wave (see SI for details). Bulk electrolysis experiments for complex $[(L1)Cu]^{2-}$ ($E_{app} = 1.3$ V at pH 11.5 with a 2.5 cm^2 ITO working electrode) show a current density of 0.11 mA/cm^2 that slowly decays to 0.06 mA/cm^2 . Simultaneous measurement of the oxygen gas generated by a Clark electrode confirms the generation of dioxygen with a Faradaic efficiency close to 100%. The decrease of current intensity over time is a consequence of lower activity of the catalyst as the pH decreases, as has been shown by FOWA. Furthermore, both CV and UV–vis spectroscopy (see SI) show that the initial species are totally retained, and, in addition, restoring the initial pH by adding base restores the initial activity. Similarly, sequential base addition during bulk electrolysis experiments maintains the catalyst activity over long periods of time (1 h) without apparent losses (see SI). Further, no copper oxide adsorption at the ITO electrode surface could be detected under the present conditions, as confirmed by CV, UV–vis, and EDX analysis, evidencing the molecular nature of the electrocatalytic water oxidation.

The nature of the species generated in the catalytic cycle was also investigated by DFT calculations (B3LYP-D3 calculations with implicit SMD solvation, see SI for computational details), which nicely complement the results obtained experimentally. A complete catalytic cycle is presented in Figure 3, including the energies involved in the different steps. At oxidation state II, the catalyst remains in its resting state and is activated by two consecutive one-electron transfers, as shown by CV techniques and described in eqs 1 and 2. The computed oxidation potentials, 0.53 and 1.26 V, are in good agreement with the

experimental values of 0.56 and 1.25 V, respectively. Calculations confirmed the radical cationic ligand nature of species C, as the attempts to obtain a Cu(IV) species always reverted to the Cu(III) complex with internal electron transfer from the ligand (Figure S27).

Species C, $[(L1^{\bullet})Cu(III)(OH)]$, reacts with an additional OH^- from the media to ultimately produce intermediate E (see Figure 3) with a peroxo unit, $[(L1)Cu(II)(HO-OH)]$, as usually assumed in this type of chemistry following a concerted two-electron step.^{5b,11} However, it follows an unusual path that deserves some comment.

In the usual water nucleophilic attack (WNA) pathway, the OH^- would directly attack the O and form the O–O bond in a single step through a moderate energy transition state. Our attempts to locate such a transition state failed, revealing instead the more complex picture indicated in Figure 4. There

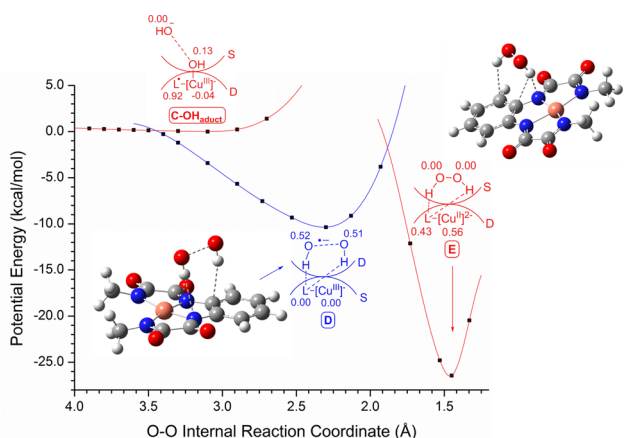


Figure 4. Potential energy relaxed scan for the O–O bond formation. The energy barrier for the second I_{SET} is estimated from changes of potential energy in the coordinate scan.

is no direct connection between species C and E (the two curves in red) through a two-electron transfer. Instead, they are connected through an additional electronic state, shown in blue in the figure. This electronic state, which we have labeled as species D, results from C by transfer of one electron from the incoming OH^- to the $[(L1^{\bullet})Cu(III)]$ moiety (initially in a doublet state) to form a $(HO\cdots OH)^{\bullet-}$ radical anion fragment with a partial O–O bond (doublet state, with an O \cdots O distance of 2.3 Å) and hydrogen bonded to the $[(L1)Cu(III)]$ complex (H-bonding distances between 2.5 and 2.9 Å, see SI). D then evolves to E through a second electron transfer, converting the HO–OH unit to a singlet state and the $[(L1)Cu(II)]$ unit to a doublet. In species E, the HO–OH fragment is again strongly hydrogen bonded to the $[(L1)Cu(II)]$ moiety (see SI). We propose to label this type of mechanism as single-electron-transfer water nucleophilic attack (SET-WNA), differing from the traditional WNA, where the two electrons are transferred in a single step. Of course, this SET-WNA mechanism would be impossible in the absence of a transition metal able to undergo a fast single electron transfer toward the HO–OH moiety formation. The generation of hydroxyl radical species would otherwise be prohibitively high. Thus, in this new SET-WNA mechanism, the O–O bond formation step can be considered to involve two consecutive intramolecular single electron transfer (I_{SET}) steps. Another interesting particularity of our SET-WNA mechanism proposed here is the absence of a direct

Cu–O bond in species D and E; instead, the $(HO\cdots OH)^{\bullet-}$ and $(HO-OH)^{2-}$ moieties are bonded to the $[(L1)Cu]^{2-}$ metal complex via hydrogen bonding, as has been already indicated above. Precedent for intramolecular ligand-based hydrogen bonding has been reported recently for related Fe complexes.¹² In our case, the SET-WNA mechanism has the important consequence of allowing the O–O bond formation with a very low barrier of 5.5 kcal/mol, thus practically instantaneously after species C is formed by oxidation at the electrode in the presence of a basic solution. The evolution from E to dioxygen release and recovery of catalyst A follows a more conventional pathway, which is discussed in detail in the SI, although it is worth mentioning that the $[(L1)Cu(II)-(HOOH)]$ complex E is first oxidized to the corresponding $[(L1)Cu(III)(HOOH^{\bullet})]$ species by a metal-based electron transfer at a potential of 0.63 V. Then, a proton-coupled electron transfer happens at a potential of 0.42 V, resulting in the formation of a $[(L1)Cu(III)(HOO^{\bullet})]$ complex which evolves dioxygen and a free proton. These values indicate that those two processes experimentally occur in a single step involving two electrons and one proton.

As evidenced by CV and confirmed by DFT, the rds involves the generation of the radical cation species C and its reaction with OH^- . It is thus reasonable that electronic perturbation of the aromatic ring should strongly influence both thermodynamics and kinetics of the water oxidation reaction catalyzed by this type of complexes. For this purpose, we have prepared a family of copper complexes containing electron-donating groups such as Me and OMe in the aromatic ring, as indicated in Figure 1. The CV depicted in Figure 2 clearly shows how the onset of the catalytic wave is shifted to the cathodic region as a function of the strength of the electron-donating group. In particular, it is impressive to see that, for complex $[(L4)Cu]^{2-}$, the overpotential at which water oxidation occurs is 530 mV lower than for $[(L1)Cu]^{2-}$ and is situated at only 170 mV above the thermodynamic value. This is the first example in the literature where a rational ligand variation allows us to exert such a degree of control over the electrocatalytic water oxidation overpotential, driving it to a record low for first-row transition metal complexes.¹³

A set of electrochemical parameters and kinetic data is presented in Table 1, together with related data for other Cu complexes described previously in the literature.^{8b,14} It is interesting to observe that, for $[(L1)Cu]^{2-}$ and $[(L2)Cu]^{2-}$ (entries 1 and 2, Table 1), the rate constants are 3.56 and 3.58 s^{-1} , respectively, whereas for $[(L3)Cu]^{2-}$ and $[(L4)Cu]^{2-}$ (entries 3 and 4, Table 1), the rate constants decrease by 1 order of magnitude, suggesting an important involvement of the electron-transfer process at the rds and a significant stabilization of the radical cation active species. On the other hand, increasing the pH from 11.5 to 12.5 increases the rate constant up to 11.96 s^{-1} . It is also important to realize here that, as the strength of the electron-donating group increases, the oxidative ruggedness of the radical cation species decreases, manifesting the existence of a decomposition pathway coupled to the water oxidation catalysis for complexes $[(L3)Cu]^{2-}$ and $[(L4)Cu]^{2-}$. We are focusing at present on ligand design to improve oxidative stability. Nevertheless, $[(L1)Cu]^{2-}$ is the most oxidatively rugged Cu-based WOC reported to date, as judged electrochemically by the charge under the III/II redox wave before and after the electrocatalytic wave (see SI). The fastest Cu-based WOC complex reported, $[(bpy)Cu(OH)_2]$, works under an overpotential of 750 mV at pH 12.5 (see entry

Table 1. Kinetic and Electrochemical Data of Complexes [(LY)Cu]²⁻ (Y = 1–4) and Related Cu Complexes Described in the Literature That Have Been Reported To Act as Water Oxidation Catalysts

entry ^a	catalyst ^b	pH	η , mV ^c	k_{obs} , s ⁻¹ ^d
1 ^{tw}	[(L1)Cu] ²⁻	11.5	700	3.56 ^e
2 ^{tw}	[(L2)Cu] ²⁻	11.5	400	3.58
3 ^{tw}	[(L3)Cu] ²⁻	11.5	270	0.43
4 ^{tw}	[(L4)Cu] ²⁻	11.5	170	0.16
5 ^{14c}	[(Py ₃ P)Cu(OH)] ⁻	8.0	~500	20
6 ^{14g}	[(dhbp)Cu(OH) ₂]	12.4	~540	0.4
7 ^{14a}	[(bpy)Cu(OH) ₂]	12.5	750	100
8 ^{14d}	[Cu ₂ (BPMAN)(μ -OH)] ³⁺	7.0	~1050	0.6

^atw = this work. ^bPy₃P = N,N-bis(2-(2-pyridyl)ethyl)pyridine-2,6-dicarboxamide; dhbp = 6,6'-dihydroxy-2,2'-bpy; bpy = 2,2'-bpy; bpmn = 2,7-[bis(2-pyridylmethyl)aminomethyl]-1,8-naphthyridine. ^cMeasured by DPV for entries 1–4 and 8 and from the initial foot of the electrocatalytic wave or the half-peak potential for CVs for the rest. ^dMeasured by FOWA in complexes [(LY)Cu]²⁻ and other methodologies for the other complexes. ^e k_{obs} = 11.96 at pH 12.5.

8, Table 1), whereas the complex [(Py₃P)Cu(OH)]⁻ (entry 5, Table 1) has been reported to work at pH 8.0 with a rate constant of 20 s⁻¹ and an overpotential of approximately 500 mV. Finally, a dinuclear complex, [Cu₂(BPMAN)(μ -OH)]³⁺ (entry 8, Table 1), has been reported that works at pH 7, is relatively slow, 0.6 s⁻¹, and works under an overpotential of 1050 mV. Clearly, more molecular Cu-based WOCs are needed in order to understand the factors that allow us to rationally build fast complexes with oxidatively rugged ligands that work ideally at pH 7 and with low overpotentials.

In conclusion, we have prepared a family of Cu complexes that are capable of oxidizing water to dioxygen and whose rate-determining step involves the redox activity of the ligand. Further fine-tuning of the ligand backbone allows reducing the overpotential for water oxidation in this family of complexes by more than 500 mV, all the way to a record low overpotential of 170 mV. In addition, DFT analysis puts forward an unprecedented pathway where the O–O bond formation occurs in a two-step, one-electron processes and where the peroxo intermediate generated has no formal M–O bond, in sharp contrast with the previous mechanism described in the literature.¹¹ The interplay between electrons being removed from the metal and/or the ligands opens up new avenues for molecular water oxidation catalyst design. We are at present focusing our attention on developing further families of molecular water oxidation catalysts based on redox non-innocent and oxidatively rugged ligands.

■ ASSOCIATED CONTENT

● Supporting Information

Procedures, crystallographic data, and Cartesian coordinates. The Supporting Information is available free of charge on the ACS Publications website at DOI: 10.1021/jacs.5b03977.

■ AUTHOR INFORMATION

Corresponding Authors

*fmaseras@iciq.es

*allobet@iciq.es

Notes

The authors declare no competing financial interest.

■ ACKNOWLEDGMENTS

We thank MINECO (CTQ2014-57761-R, CTQ-2013-49075-R, SEV-2013-0319, CTQ2014-52974-REDC), the ICIQ Foundation, and the EU COST actions CM1202 and CM1205. I.F.-A. also thanks the Severo Ochoa pre-doctoral training fellowship (Ref: SVP-2014-068662). P.G.-B. thanks “La Caixa” Foundation for a Ph.D. grant.

■ REFERENCES

- (1) Berardi, S.; Drouet, S.; Francas, L.; Gimbert-Surinach, C.; Guttentag, M.; Richmond, C.; Stoll, T.; Llobet, A. *Chem. Soc. Rev.* **2014**, *43*, 7501.
- (2) (a) Melis, A. *Energy Environ. Sci.* **2012**, *5*, 5531. (b) Alstrum-Acevedo, J. H.; Brennaman, M. K.; Meyer, T. J. *Inorg. Chem.* **2005**, *44*, 6802. (c) Nocera, D. G. *Acc. Chem. Res.* **2012**, *45*, 767.
- (3) Cox, N.; Pantazis, D. A.; Neese, F.; Lubitz, W. *Acc. Chem. Res.* **2013**, *46*, 1588.
- (4) (a) Zhou, J.; Xi, W.; Hurst, J. K. *Inorg. Chem.* **1990**, *29*, 160. (b) Radaram, B.; Ivie, J. A.; Singh, W. M.; Grudzien, R. M.; Reibenspies, J. H.; Webster, C. E.; Zhao, X. *Inorg. Chem.* **2011**, *50*, 10564. (c) Hong, D.; Mandal, S.; Yamada, Y.; Lee, Y.-M.; Nam, W.; Llobet, A.; Fukuzumi, S. *Inorg. Chem.* **2013**, *52*, 9522.
- (5) (a) Wang, D.; Ghirlanda, G.; Allen, J. P. *J. Am. Chem. Soc.* **2014**, *136*, 10198. (b) Karlsson, E. A.; Lee, B.-L.; Åkermark, T.; Johnston, E. V.; Kärkäs, M. D.; Sun, J.; Hansson, Ö.; Bäckvall, J.-E.; Åkermark, B. *Angew. Chem., Int. Ed.* **2011**, *50*, 11715. (c) Crabtree, R. H. *Chem. Rev.* **2015**, *115*, 127.
- (6) (a) Muckerman, J. T.; Polyansky, D. E.; Wada, T.; Tanaka, K.; Fujita, E. *Inorg. Chem.* **2008**, *47*, 1787. (b) Boyer, J. L.; Rochford, J.; Tsai, M.-K.; Muckerman, J. T.; Fujita, E. *Coord. Chem. Rev.* **2010**, *254*, 309.
- (7) (a) Chirik, P. J.; Wieghardt, K. *Science* **2010**, *327*, 794. (b) Choudhuri, M. M. R.; Kaim, W.; Sarkar, B.; Crutchley, R. J. *Inorg. Chem.* **2013**, *52*, 11060.
- (8) (a) Ruiz, R.; Surville-Barland, C.; Aukauloo, A.; Anxolabehere-Mallart, E.; Journaux, Y.; Cano, J.; Carmen Munoz, M. *J. Chem. Soc., Dalton Trans.* **1997**, 745. (b) Fu, L.-Z.; Fang, T.; Zhou, L.-L.; Zhan, S.-Z. *RSC Adv.* **2014**, *4*, 53674.
- (9) Ottenwaelder, X.; Aukauloo, A.; Journaux, Y.; Carrasco, R.; Cano, J.; Cervera, B.; Castro, I.; Curreli, S.; Munoz, M. C.; Rosello, A. L.; Soto, B.; Ruiz-Garcia, R. *Dalton Trans.* **2005**, 2516.
- (10) Costentin, C.; Drouet, S.; Robert, M.; Savéant, J.-M. *J. Am. Chem. Soc.* **2012**, *134*, 11235.
- (11) Sala, X.; Maji, S.; Bofill, R.; García-Antón, J.; Escriche, L.; Llobet, A. *Acc. Chem. Res.* **2014**, *47*, 504.
- (12) Bichler, B.; Glatz, M.; Stoger, B.; Mereiter, K.; Veiros, L. F.; Kirchner, K. *Dalton Trans.* **2014**, *43*, 14517.
- (13) (a) Ellis, W. C.; McDaniel, N. D.; Bernhard, S.; Collins, T. J. *J. Am. Chem. Soc.* **2010**, *132*, 10990. (b) Liao, R.-Z.; Li, X.-C.; Siegbahn, P. E. M. *Eur. J. Inorg. Chem.* **2014**, 728.
- (14) (a) Barnett, S. M.; Goldberg, K. I.; Mayer, J. M. *Nat. Chem.* **2012**, *4*, 498. (b) Zhang, M.-T.; Chen, Z.; Kang, P.; Meyer, T. J. *J. Am. Chem. Soc.* **2013**, *135*, 2048. (c) Coggins, M. K.; Zhang, M.-T.; Chen, Z.; Song, N.; Meyer, T. J. *Angew. Chem., Int. Ed.* **2014**, *53*, 12226. (d) Su, X.-J.; Gao, M.; Jiao, L.; Liao, R.-Z.; Siegbahn, P. E. M.; Cheng, J.-P.; Zhang, M.-T. *Angew. Chem., Int. Ed.* **2015**, *54*, 4909. (e) Pap, J. S.; Szyrwiel, L.; Sranko, D.; Kerner, Z.; Setner, B.; Szewczuk, Z.; Malinka, W. *Chem. Commun.* **2015**, *51*, 6322. (f) Gerlach, D. L.; Bagan, S.; Cruce, A. A.; Burks, D. B.; Nieto, I.; Truong, H. T.; Kelley, S. P.; Herbst-Gervasoni, C. J.; Jernigan, K. L.; Bowman, M. K.; Pan, S.; Zeller, M.; Papish, E. T. *Inorg. Chem.* **2014**, *53*, 12689. (g) Zhang, T.; Wang, C.; Liu, S.; Wang, J.-L.; Lin, W. *J. Am. Chem. Soc.* **2014**, *136*, 273.